Article

Journal of
Biomedical Nanotechnology
Vol. 14, 1627–1634, 2018
www.aspbs.com/jbn

Copyright © 2018 American Scientific Publishers
All rights reserved
Printed in the United States of America

Nitrogen-Incorporated Ultrananocrystalline Diamond Electrodes for Dopamine Determination

Pei-Ling Jiang[1], Ping-Yen Hsieh[1], Ying-Chieh Chen[1,*], Chi-Young Lee[1], Hwan-You Chang[2], and Nyan-Hwa Tai[1,*]

[1] *Department of Materials Science and Engineering, National Tsing-Hua University, Hsinchu, 300, Taiwan*
[2] *Department of Life Science, National Tsing-Hua University, Hsinchu, 300, Taiwan*

In this paper, nitrogen incorporated ultrananocrystalline diamond (NUNCD) films were fabricated for use as electrodes to detect dopamine. The NUNCD electrodes achieved high sensitivity, great selectivity, and excellent detection limits for dopamine sensing. The NUNCD electrode, fabricated as a potential sensitive biosensor for dopamine without any catalyst or mediators, demonstrated good activity for the direct detection of dopamine by simply putting the bare NUNCD electrode into a dopamine solution. Furthermore, the marked selectivity of the NUNCD electrode is very favorable for the determination of dopamine (DA) concentration (0.32 μM) in the presence of ascorbic acid (AA) and uric acid (UA). Considering dopamine detection in real biological fluid samples, the NUNCD electrode performed excellently with a detection limit of 0.39 μM and a high recovery ranging from 90–120%, revealing that NUNCD electrodes have promising use in the sensing of dopamine.

KEYWORDS: *Nitrogen Incorporated Ultrananocrystalline Diamond (NUNCD), Dopamine Sensing, Electrode.*

INTRODUCTION

Dopamine (DA) is a catecholamine neurotransmitter that is commonly found in the nervous systems of mammals. Dopamine modulates the functions of the hormonal, renal, cardiovascular, and central nervous systems, and controls movement, metal state, and behavior. The normal level of dopamine in human serum is 0.01–0.1 μM.[1] An excess level of dopamine is related to some biological diseases such as Huntington's disease, neuroblastoma, or schizophrenia. A deficit in dopamine concentration is associated with Parkinsonism, Alzheimer's disease, epilepsy, attention deficit hyperactivity disorder, and restless legs syndrome.[2,3] Thus, dopamine could act as a biomarker for these diseases. The release of dopamine from a dopaminergic neuron is rapid and the amount released is quite tiny, so the detection of dopamine must be rapid and requires ultra-sensitivity.

Conventional dopamine sensing methods, like high performance liquid chromatography—mass spectrometry, immunosensing microfluidic systems, and spectrophotometry, have achieved good sensitivity and detection limits. However, the complicated and high-cost instruments used in these methods limit their application. Recently, the electrochemical method has been extensively researched for use in dopamine detection, since it is cost-effective, possesses a short analysis time, and is easy to operate.[4] However, the use of the electrochemical method for detecting dopamine faces some challenges. Firstly, the interference effect may hinder the dopamine signal. Since the electrochemical method employs the electroactive property of dopamine, which oxidizes at a positive potential and reduces at a negative potential, to detect it, the coexisting biomolecules in the serum would influence the signal of the dopamine. In particular, ascorbic acid and uric acid, the coexisting electroactive species, provide signals that would merge with the dopamine signal when a bare electrode, like glassy carbon, is used.[5–7] Secondly, the electrode may encounter a biofilm-fouling problem, thereby deteriorating its performance.[1,8] The adsorbed oxidized bimolecular products on the electrode surface result in a decrease in sensitivity by decreasing the electroactive sites. In order to overcome this problem, some scientists employ modified nanostructures, like metal

*Authors to whom correspondence should be addressed.
Emails: yisschen@mx.nthu.edu.tw, nhtai@mx.nthu.edu.tw
Received: 6 September 2017
Revised/Accepted: 4 December 2017

nanoparticles,[2] carbon nanotubes,[9] and graphene,[10–13] in order to increase the amount of catalytic sites on the electrode. Other approaches examined include polymers,[14] poly(ionic liquids),[15] or selective membranes[16] to enhance the selectivity of the electrodes. However, it usually requires lots of time, money, and effort in order to fabricate electrodes with nanostructures, and the modifiers are more likely unstable and easily detachable from the electrode surface during measurement.

Nitrogen incorporated ultrananocrystalline diamond (NUNCD) films exhibit the excellent properties of diamond, such as a wide working potential window, low background current, high chemical inertness, and high hardness.[17–19] In addition, through the incorporation of nitrogen into the grain boundary, the NUNCD films could have a high conductivity.[20,21] The synthesis process is also quite short (∼4 hrs), which is beneficial for commercial use. Moreover, NUNCD films do not require a modification process; this is beneficial because the modification may detach from the bare electrode and affect the sensing performance after extensive usage. In our previous study,[21] NUNCD films show excellent electrocatalytic activity (0.5–500 μM) for sensing dopamine in the presence of ascorbic acid (AA). To being the biosensor with higher sensitivity and reliability, direct sensing dopamine in real samples, like serum is necessary. In this study, NUNCD grown in nitrogen-rich plasma under bias condition reach higher detection sensitivity for dopamine and the[22] limit of detection can be as low as 0.32 μM in the presence of more interference or in the serum *ex vivo*.

EXPERIMENTAL DETAILS

Chemicals

Nano-diamond powder (∼100 nm) was bought from FACT. Titanium powder (∼325 mesh) was obtained from Alfa Aesar. Ascorbic acid (AA), dopamine (DA), uric acid (UA), phosphate buffer solution (PBS, 1 M, pH 7.4), and potassium hydroxide (KOH) were purchased from Sigma-Aldrich. Secondary distilled water was used to dilute PBS. The AA, DA, and UA solutions were freshly prepared in 0.1 M PBS.

Synthesis of Diamond Films

The NUNCD and UNCD films were synthesized on the *n*-type Si substrate using microwave plasma enhanced chemical vapor deposition (MPECVD). The Si substrates were then immersed in a 200 ml methanol solution that contained 200 mg nano-diamond powder and 200 mg titanium powder to create nucleation sites. The pretreated samples were put onto the holder in the MPECVD chamber. The synthesis conditions for producing the NUNCD film was 94% N_2/6% CH_4 gas at 1400 W and 50 torr using a −300 V substrate bias for 1 hour. The UNCD films were grown under 99% Ar/1% CH_4 gas at 1200 W and 120 torr without any substrate bias for 1 hour.

Analysis Instrument

The surface morphology of the films was characterized by field emission scanning electron microscopy (FESEM, JEOL JSM 6500F). The bonding structures of the films were analyzed by Raman spectroscopy (Raman, Horiba Jobin Yvon LABRAM HR 800 UV) and X-ray photoelectron spectroscopy (XPS, ULVAC-PHI PHI 5000 Versaprobe II). The resistivity of the films was measured by Hall measurements in a van der Pauw configuration.

Electrochemical Measurement

The electrochemical measurement was conducted using a potentiostat (600C series, Autolab), and the three-electrode system was adopted: the reference electrode, counter electrode, and working electrode were Ag/AgCl, Pt wire, and the fabricated NUNCD film, respectively. The cyclic voltammetry (CV) was used to analyze the electrochemical properties of the electrode toward AA, DA, and UA. The differential pulse voltammetry (DPV) was applied to detect the dopamine content in the samples. The analyte volume was 2 ml, and the working electrode was washed with ethanol, KOH, and DI water after each scan.

RESULTS AND DISCUSSION

Surface Morphology of the Diamond Films

The FESEM images in Figure 1 reveal the morphology of the UNCD film and the NUNCD film. The top view of the UNCD film shown in Figure 1(a) indicates that the film consists of continuous equiaxed grains. Under an argon-enriched environment, the growing species is C_2, and the second nucleation rate is higher than that of the hydrogen-enriched plasma; this produces grains which are several nanometers in size. Figure 1(b) shows the top view of the NUNCD film. The synthesis conditions were 94% N_2/6% CH_4 gas, and it was found that the CN species would dissociate in the plasma under the influence of an applied bias. The bonding strength of the dissociated CN species was found to be strong, providing a template for the anisotropic growing of the grains.[23,24] The needle-like grains are encapsulated by a graphitic phase of grain boundaries, which enhance the conductivity of the NUNCD films. The resistivity of the films was measured using Hall measurements. The resistivity of the UNCD films is on the order of MΩ·cm, but after incorporating nitrogen into films the resistivity of NUNCD film significantly decreased to 63.15 $\mu\Omega\cdot$cm, which was high enough to permit its use as an electrode for electrochemical sensing.

Raman Analysis of the Diamond Films

Raman spectroscopy is a common tool used to analyze carbonic materials, providing information like chemical structure, vibration and stretching modes, and composition. Figure 2 shows the Raman spectrum of the UNCD and NUNCD films. The characterized peaks located at

Delivered by Ingenta

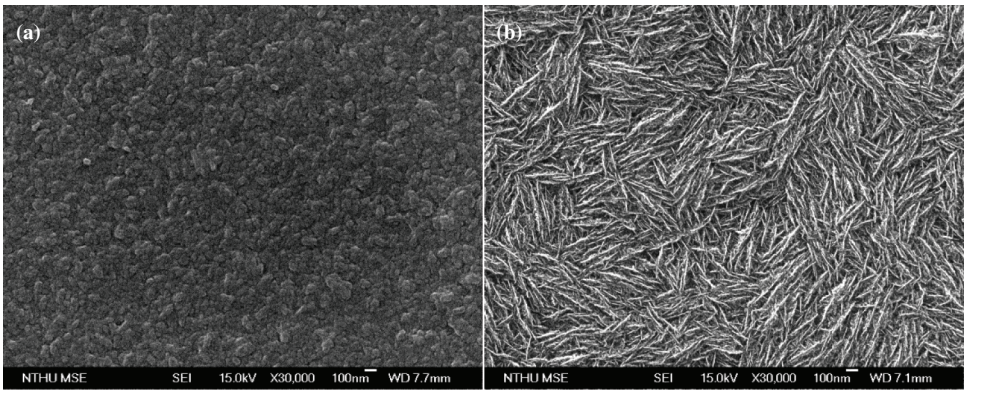

Figure 1. **FESEM images of the (a) UNCD and (b) NUNCD films grown for 1 hr.**

1160 cm^{-1}, 1332 cm^{-1}, 1350 cm^{-1}, and 1580 cm^{-1} are referred to as the υ_1 band resonance peak, diamond characterization peak, D band resonance peak, and G band resonance peak, respectively. The υ_1 band resonance peak originates from trans-polyacetylene.[25–27] The diamond peak is related to the sp^3 bonding structure and is in the T_{2g} mode. The D band is the A_{1g} breathing mode of the sp^2 atoms in the ring, which represents the disordered carbons. The G band results from the E_{2g} stretching mode of all sp^2 sites.[28,29] Compared to the Raman spectrum of the UNCD films in curve (a), which were deposited without nitrogen, the typical Raman spectrum of the NUNCD films, synthesized under nitrogen plasma, is shown in Figure 2 curve (b). By incorporating nitrogen into the film, the position of the D band shifted from 1350 cm^{-1} to 1425 cm^{-1} and the G band shifted from 1580 cm^{-1} to 1590 cm^{-1}, which is a result of the increasing graphitic phase. In addition, the diamond characteristic peak and υ_1 band resonance peak were shown to be suppressed with the incorporation of nitrogen, which is due to the larger graphitic content in the NUNCD films. The blue shift of the sp^2-related resonance peaks, the unobvious diamond characteristic peak, and the υ_1 band resonance peak reflect the increasing graphitic phase content, and this contributes to the high conductivity of the NUNCD films.

IP: 178.57.67.42 On: Sat, 02 Feb 2019 10:01:20
Copyright: American Scientific Publishers
Delivered by Ingenta

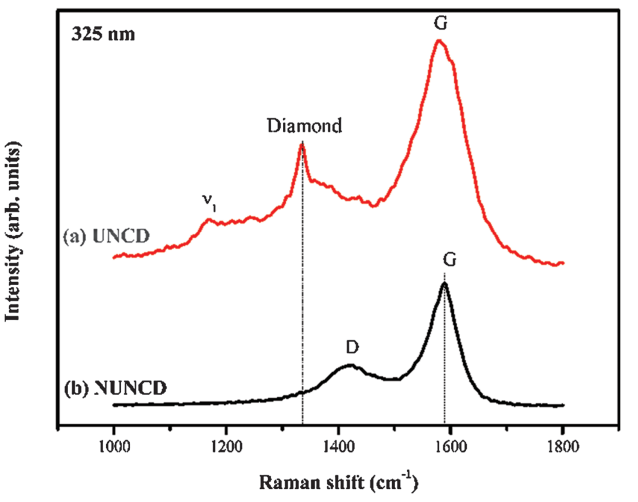

Figure 2. **Raman spectra of UNCD (curve a) and NUNCD (curve b) films.**

XPS Analysis of NUNCD

The chemical composition of the NUNCD films was investigated by XPS, and the corresponding XPS spectra are shown in Figure 3. The XPS survey spectrum (Fig. 3(a)) revealed only the presence of carbon atoms in the NUNCD films. The C1*s* peak located at 285 eV resulted from the Lorentzian peaks at binding energies of 284.48 eV, 285.34 eV, 285.84 eV, and 286.29 eV for sp^2 C═C, sp^3 C═C, sp^2 C═N, and sp^3 C–N, respectively. The relative peak intensity of sp^2 C═C to the total carbon-based phase is about 57.11%, indicating that a large amount of graphitic phase was present in the NUNCD films. In addition, the presence of a sp^2 C═N and a sp^3 C–N peak reflect that N atoms have successfully been incorporated into the NUNCD films.

OES Analysis of Plasma

The chemical species in the plasma were monitored and recorded by optical emission spectroscopy (OES) under varied substrate biases (Fig. 4(a)) and chamber pressures (Fig. 4(b)). The CN violent system (~388.69 nm and ~421.00 nm) and C_2 swan system (~472.81 nm and ~517.57 nm) are observed in the spectrum, indicating that the CN and C_2 growth species are contained in the N_2/CH_4 plasma. The C_2 species contributed to the growth of the diamond, and the CN species provided the template for anisotropic growth, resulting in the needle-like structure of NUNCD grains. Altering the pressure in the chamber or the applied bias did not change the OES spectrum.

Electrochemical Properties of the Electrode

The electrochemical behavior of the NUNCD electrode for use in detecting AA, DA, and UA was investigated

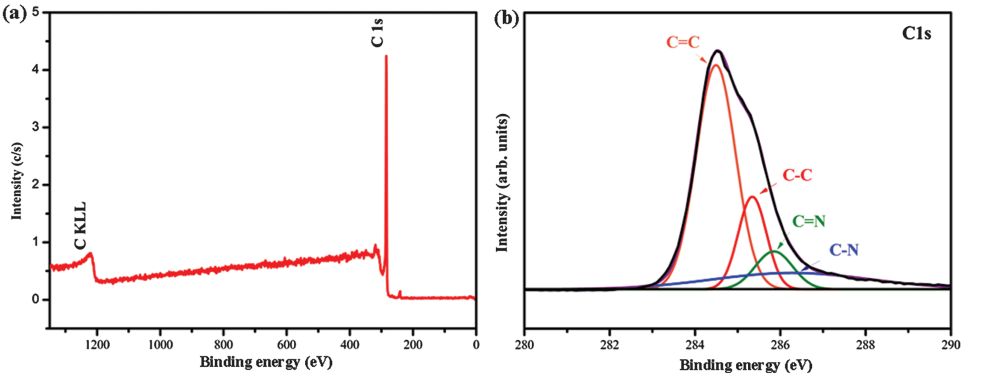

Figure 3. **(a) XPS survey spectrum and (b) high-resolution scan spectrum over C1*s* for the NUNCD film.**

by cyclic voltammetry. Some redox couples are shown in Figure 5(a). The peaks at −0.03 V, 0.15 V, and 0.28 V are in reference to the oxidation signals of AA, DA, and UA, respectively. The oxidation peak current was found to have increased with an increasing scan rate. Moreover, Figures 5(b)–(d) indicate the peak currents of AA, DA, and UA are proportional to the square root of the scan rate. This relationship is considered to be the diffusion-controlled mechanism that is accounted for by the Cottrell equation, and the current was found to be limited by the diffusion of the analyte species onto the electrode surface. In this situation, the CV experiment only sampled a small portion of the solution, i.e., the diffusion layer at the surface of the NUNCD film, which implies that the surface properties of the NUNCD film dominates the sensitivity of the electrodes.

DPV Response of Dopamine

Differential pulse voltammetry (DPV) was employed to detect dopamine due to the advantage it possesses of a lower IR drop and a non-Faradaic current, having a higher signal to noise ratio in comparison with other voltammetry methods. The NUNCD films were used as working electrodes to detect dopamine in PBS by DPV. Figure 6(a) shows the results of these experiments, wherein the oxidation peak of dopamine was found to exist at 0.13 V. A larger amount of dopamine content in the PBS results in a larger dopamine oxidation peak current, and there exists two linear relationships between these properties as shown in Figure 6(b). The linear regression equations are expressed as $I_p\ (\mu A) = 5.23 + 3.41 C_{DA}$ (μM) $(R^2 = 0.99035)$ over the range from 0.38 μM to 12.38 μM, and $I_p\ (\mu A) = 5.23 + 3.41 C_{DA}\ (\mu M)$ $(R^2 = 0.99733)$ over the range from 12.38 μM to 33 μM. The corresponding sensitivity for dopamine was found to be 3.41 μA/μM and 1.30 μA/μM, respectively, for these two regions. The adsorption strength at a higher dopamine content differed from that at lower dopamine content, resulting in the two different sensitivities of the electrode.[30] Figures 7(a) and (b) illustrate the adsorption mechanism of the lower dopamine content and higher dopamine content solutions at the NUNCD electrode, respectively. At a lower concentration, all of the biomolecules adsorb onto the electrode easily through first layer adsorption, which belongs to the monolayer adsorption mechanism. At higher concentration, however, some biomolecules need to cross the first layer biomolecules in order to adsorb onto the

Copyright: American Scientific Publishers
Delivered by Ingenta

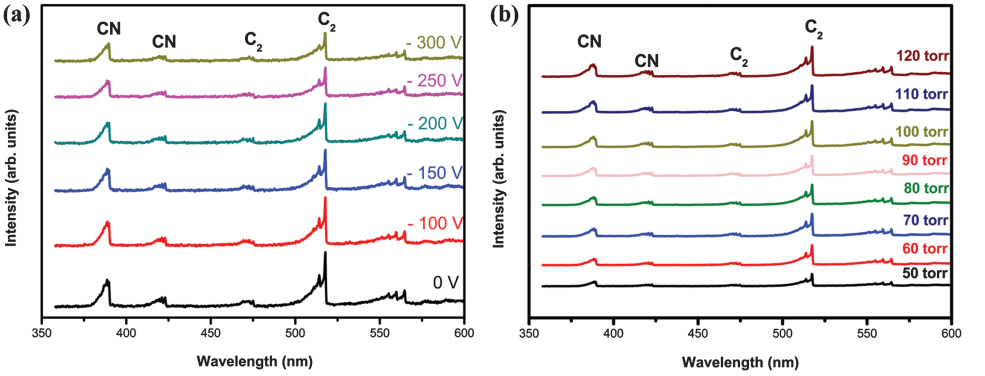

Figure 4. **Optical emission spectra of the NUNCD films at different (a) substrate biases, and (b) chamber pressures.**

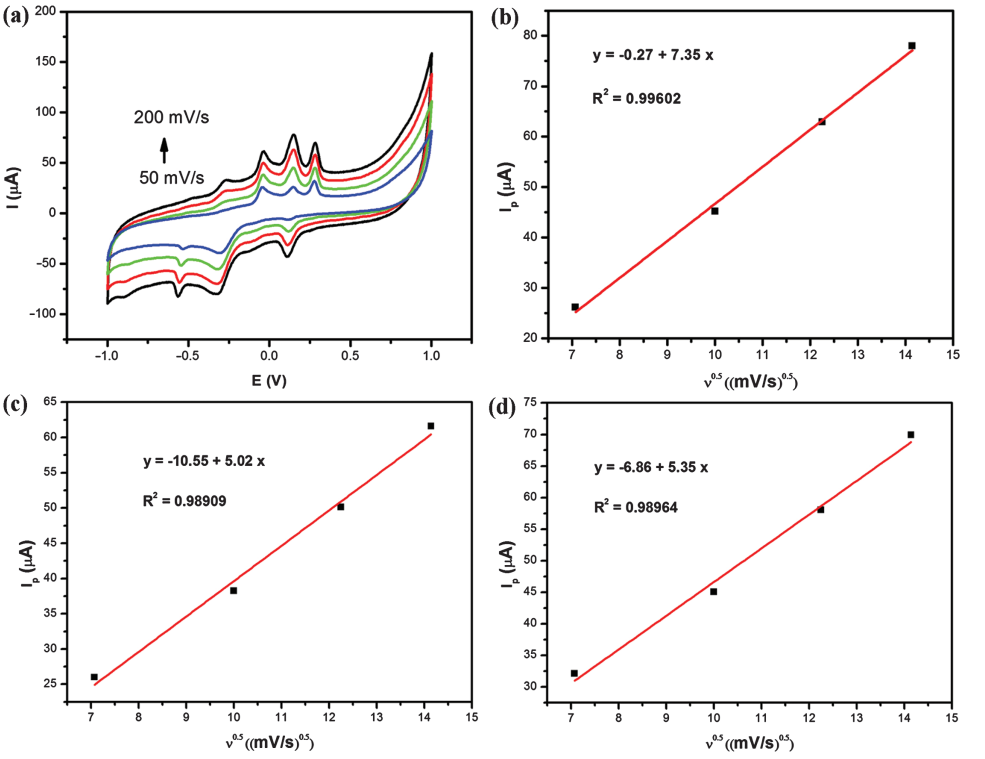

Figure 5. **(a) Cyclic voltammetry for 330 μM AA, 33 μM DA, and 33 μM UA in PBS (pH 7.4) using the NUNCD electrode. The relationship of the oxidant peak currents of (b) DA, (c) AA, and (d) UA with the square root of the scan rate.**

IP: 178.57.67.42 On: Sat, 03 Feb 2018 10:01:20
Copyright: American Scientific Publishers
Delivered by Ingenta

electrode, resulting in lower adsorption strength due to the multilayer adsorption. The weaker adsorption strength resulted in a lower sensitivity at higher dopamine content. The detection limit is estimated to be 0.32 μM ($S/N = 3$). The analytic results are listed in Table I.

Interference Test

Coexisting electroactive species, such as AA and UA, may hinder and interfere with the performance of the electrode in sensing dopamine. As such, 330 μM of AA and 33 μM of UA were added to dopamine solution in order to examine the performance of the NUNCD electrode under these conditions. The DPV results are displayed in Figure 6(c), exhibiting three distinguishable peaks at -0.06 V, 0.13 V, and 0.27 V, which are assigned to the oxidation peaks of AA, DA, and UA, respectively. The presence of AA and UA are shown to have no effect on the peak potential of DA, which had the same value of 0.13 V that was observed when sensing only dopamine. The large peak separation indicates that the NUNCD electrode possesses great selectivity toward AA, DA, and UA. Following this, the dopamine concentration was increased from 0 to 33 μM in the presence of 330 μM AA and 33 μM UA. (Fig. 6(d)). The oxidation peak current of the dopamine increased with an increasing amount of dopamine. Owing to different adsorption mechanisms at each biomolecular content range, the sensitivity of the NUNCD electrode toward DA decreased at a higher DA concentration. The sensitivity of the NUNCD electrode toward DA at 0.38–8.25 μM was 4.79 μA/μM and the sensitivity at 0.38–33 μM was 1.61 μA/μM. The linear regression equations are expressed as I_p (μA) $= 12.93 + 4.79C_{DA}$ (μM) ($R^2 = 0.98432$) over the range from 0.38 μM to 8.25 μM, and I_p (μA) $= 38.48 + 1.61C_{DA}$ (μM) ($R^2 = 0.95965$) over the range from 8.25 μM to 33 μM. The detection limit was estimate to be 0.32 μM. The analytic results are listed in Table I.

Real Sample Analyses

To evaluate the feasibility of using a NUNCD electrode for DA sensing in a bio-mimetic and biological environment, fetal bovine serum was used. The dopamine was added in the diluted fetal bovine serum in quantities from 0 to 33 μM, and the DPV results are shown in Figure 6(e). The overall response currents were found to have decreased because of the matrix effects of other substances present in the fetal bovine serum. The relationship between the dopamine oxidation current and its concentration is shown in Figure 6(f). There are two linear ranges at 0.77–8.25 μM and 8.25–33 μM, where the regression equations are I_p (μA) $= 5.23 + 3.41C_{DA}$ (μM) ($R^2 = 0.99035$) and I_p (μA) $= 30.12 + 1.30C_{DA}$ (μM) ($R^2 = 0.99733$), respectively. The respective sensitivities are about 1.25 μA/μM (0.77–8.25 μM) and 0.65 μA/μM (8.25–33 μM), which are lower than those of PBS, owing to the matrix effect of the fetal bovine serum. The detection limit was estimate to be 0.39 μM.

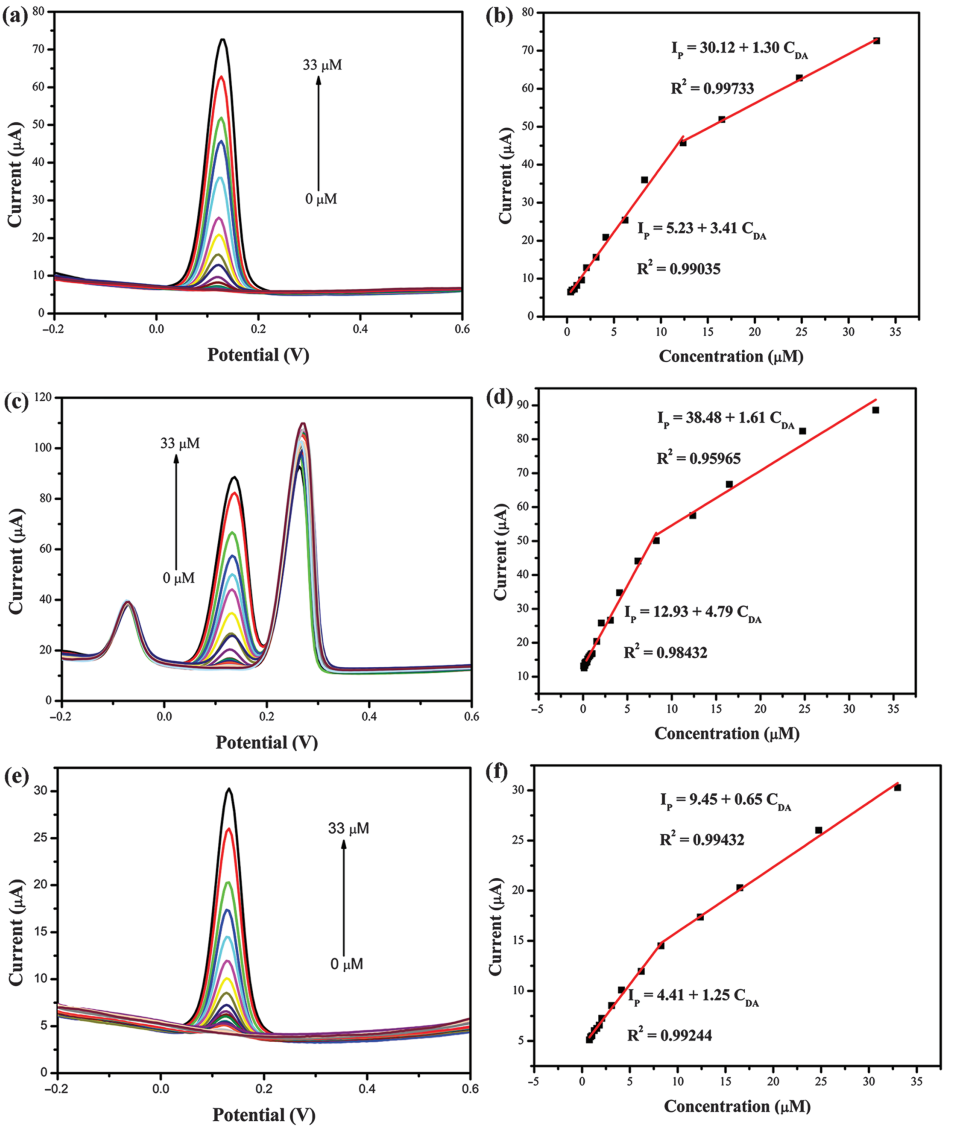

Figure 6. **NUNCD electrode detection in 0–33 μM DA in PBS (pH 7.4) by (a) DPV and (b) the calibration curve. Detection in 330 μM AA, 0–33 μM DA, and 33 μM UA in PBS (pH 7.4) by (c) DPV and (d) the calibration curve. Detection in 0–33 μM DA in FBS by (e) DPV and (f) the calibration curve.**

Dopamine Content Determination Using a Calibration Curve

The constructed calibration curve was used to determine the dopamine content in the AA, DA, and UA mixture solutions. The unknown dopamine content sample was detected via DPV in order to obtain the oxidation peak current of dopamine, which was then inputted into the calibration curve and the dopamine concentration was calculated. The determined dopamine content was compared with the value that was added. In order to evaluate the accuracy

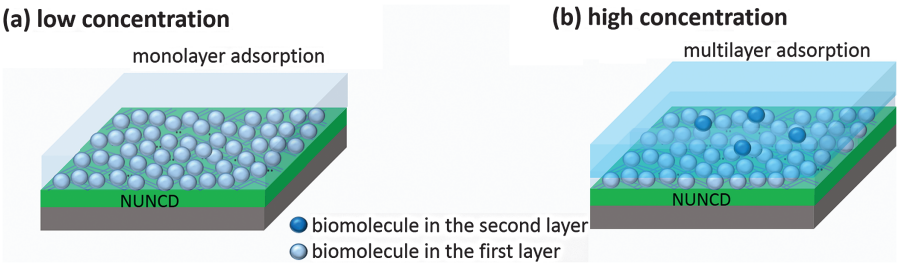

Figure 7. **Schematic of the adsorption mechanism at a (a) low concentration and (b) high concentration.**

Table I. Detection parameters of the NUNCD electrode.

Sample	Detection limit (μM)	Linear range (μM)	Sensitivity (μA/μM)
DA in PBS	0.32	0.38–12.38 12.38–33	3.41 1.30
DA, AA, UA in PBS	0.32	0.38–8.25 8.25–33	4.79 1.61
DA in FBS	0.39	0.77–8.25 8.25–33	1.25 0.65

Table II. Results of dopamine content determination in blind samples.

Sample	Added (μM)	Found (μM)	Recovery (%)
DA, AA, and UA in PBS	4.13	4.93	119.37
	8.25	8.76	106.18
	12.38	14.12	114.05
DA in FBS	4.13	3.90	94.43
	8.25	7.70	93.33
	12.38	11.64	94.06

of the NUNCD electrode toward dopamine detection, the recovery, defined as the percentage ratio of instrument-obtained value to the actual added content, was used. The results are listed in Table II. The recovery of the NUNCD electrode ranged from about 90–120%, which is promising for the detection of dopamine.

IP: 178.57.67.42 On: Sat, 02 [illegible]
Copyright: American Scientific Publishers
Delivered by [illegible]

CONCLUSIONS

In this study, as-grown NUNCD films using MPECVD and 94% N_2/6% CH_4 plasmas, were examined for their use in the selective and sensitive detection of dopamine. This was tested simply by immersing the film into a solution containing dopamine without the extra modification of the surface of the film. The NUNCD electrode with a needle-like structure exhibited high conductivity and electrochemical activity towards dopamine oxidation, even in the presence of common interferants (e.g., UA and AA). The detection limit was determined to be 0.32 μM in the controlled dopamine-containing solutions with and without interferants. Moreover, in a biological fluid, i.e., serum, the detection limit was determined to be around 0.39 μM, and the recovery was in the range of 90–120%. The application of NUNCD electrodes for dopamine oxidation and the resulting selectivity and stability were determined to be sufficient for practical dopamine detection. These promising results, combined with the biocompatibility of diamond films, make this biosensor an exceptional choice for dopamine detection *in vitro*.

Acknowledgment: This work was supported by National Tsing-Hua University under the Contract no. 105N525CE1. This study was supported by the Ministry of Science and Technology (MOST), Taiwan under project number MOST 105-2221-E-007-142.

REFERENCES

1. C. Dincer, R. Ktaich, E. Laubender, J. J. Hees, J. Kieninger, C. E. Nebel, J. Heinze, and G. A. Urban, Nanocrystalline boron-doped diamond nanoelectrode arrays for ultrasensitive dopamine detection. *Electrochim. Acta* 185, 101 **(2015)**.
2. S. Pruneanu, A. R. Biris, F. Pogacean, C. Socaci, M. Coros, M. C. Rosu, F. Watanabe, and A. S. Biris, The influence of uric and ascorbic acid on the electrochemical detection of dopamine using graphene-modified electrodes. *Electrochim. Acta* 154, 197 **(2015)**.
3. S. Hu, Q. Huang, Y. Lin, C. Wei, H. Zhang, W. Zhang, Z. Guo, X. Bao, J. Shi, and A. Hao, Reduced graphene oxide-carbon dots composite as an enhanced material for electrochemical determination of dopamine. *Electrochim. Acta* 130, 805 **(2014)**.
4. X. Zhang, S. Yu, W. He, H. Uyama, Q. Xie, L. Zhang, and F. Yang, Electrochemical sensor based on carbon-supported $NiCoO_2$ nanoparticles for selective detection of ascorbic acid. *Biosens. Bioelectron.* 55, 446 **(2014)**.
5. S. Zhou, H. Shi, X. Feng, K. Xue, and W. Song, Design of templated nanoporous carbon electrode materials with substantial high specific surface area for simultaneous determination ofbiomolecules. *Biosens. Bioelectron.* 42, 163 **(2013)**.
6. X. Zhang, L.-X. Ma, and Y.-C. Zhang, Electrodeposition of platinum nanosheets on C 60 decorated glassy carbon electrode as a stable electrochemical biosensor for simultaneous detection of ascorbic acid, dopamine and uric acid. *Electrochim. Acta* 177, 118 **(2015)**.
7. T. Qian, C. Yu, X. Zhou, P. Ma, S. Wu, L. Xu, and J. Shen, Ultrasensitive dopamine sensor based on novel molecularly imprinted polypyrrole coated carbon nanotubes. *Biosens. Bioelectron.* 58, 237 **(2014)**.
8. F. Ye, C. Feng, J. Jiang, and S. Han, Simultaneous determination of dopamine, uric acid and nitrite using carboxylated graphene oxide/lanthanum modified electrode. *Electrochim. Acta* 182, 935 **(2015)**.
9. Y. J. Yang and W. Li, CTAB functionalized graphene oxide/multiwalled carbon nanotube composite modified electrode for the simultaneous determination of ascorbic acid, dopamine, uric acid and nitrite. *Biosens. Bioelectron.* 56, 300 **(2014)**.
10. Z.-H. Sheng, X.-Q. Zheng, J.-Y. Xu, W.-J. Bao, F.-B. Wang, and X.-H. Xia, Electrochemical sensor based on nitrogen doped graphene: Simultaneous determination of ascorbic acid, dopamine and uric acid. *Biosens. Bioelectron.* 34, 125 **(2012)**.
11. H. Hu, Y. Song, M. Feng, and H. Zhan, Carbon nanomaterials for simultaneous determination of dopamine and uric acid in the presence of ascorbic acid: From one-dimensional to the quasi one-dimensional. *Electrochim. Acta* 190, 40 **(2016)**.
12. M. Hadi and A. Rouhollahi, Simultaneous electrochemical sensing of ascorbic acid, dopamine and uric acid at anodized nanocrystalline graphite-like pyrolytic carbon film electrode. *Anal. Chim. Acta* 721, 55 **(2012)**.
13. X. Yan, Y. Gu, C. Li, L. Tang, B. Zheng, Y. Li, Z. Zhang, and M. Yang, Synergetic catalysis based on the proline tailed metalloporphyrin with graphene sheet as efficient mimetic enzyme for ultrasensitive electrochemical detection of dopamine. *Biosens. Bioelectron.* 77, 1032 **(2016)**.
14. X. Liu, L. Zhang, S. Wei, S. Chen, X. Ou, and Q. Lu, Overoxidized polyimidazole/graphene oxide copolymer modified electrode for the simultaneous determination of ascorbic acid, dopamine, uric acid, guanine and adenine. *Biosens. Bioelectron.* 57, 232 **(2014)**.
15. H. Mao, J. Liang, H. Zhang, Q. Pei, D. Liu, S. Wu, Y. Zhang, and X.-M. Song, Poly(ionic liquids) functionalized polypyrrole/graphene oxide nanosheets for electrochemical sensor to detect dopamine in the presence of ascorbic acid. *Biosens. Bioelectron.* 70, 289 **(2015)**.
16. W. Zhang, J. Zheng, J. Shi, Z. Lin, Q. Huang, H. Zhang, C. Wei, J. Chen, S. Hu, and A. Hao, Nafion covered core–shell structured Fe_3O_4@graphene nanospheres modified electrode for

highly selective detection of dopamine. *Anal. Chim. Acta* 853, 285 (**2015**).

17. Q. Chen, D. M. Gruen, A. R. Krauss, T. D. Corrigan, M. Witek, and G. M. Swain, The structure and electrochemical behavior of nitrogen-containing nanocrystalline diamond films deposited from $CH_4/N_2/Ar$ mixtures. *J. Electrochem. Soc.* 148, E44 (**2001**).

18. M. Iwaki, S. Sato, K. Takahashi, and H. Sakairi, Electrical conductivity of nitrogen and argon implanted diamond. *Nuclear Instruments and Methods in Physics Research* 209, 1129 (**1983**).

19. Y. V. Pelskov, A. Y. Sakharova, M. Krotova, L. Bouilov, and B. Spitsyn, Photoelectrochemical properties of semiconductor diamond. *Journal of Electroanalytical Chemistry and Interfacial Electrochemistry* 228, 19 (**1987**).

20. K. J. Sankaran, B. R. Huang, A. Saravanan, D. Manoharan, N. H. Tai, and I. Lin, Nitrogen incorporated ultrananocrystalline diamond microstructures from bias-enhanced microwave N_2/CH_4-plasma chemical vapor deposition. *Plasma Processes and Polymers* 13, 419 (**2016**).

21. A. Saravanan, B.-R. Huang, K. J. Sankaran, N.-H. Tai, and I.-N. Lin, Highly conductive diamond-graphite nanohybrid films with enhanced electron field emission and microplasma illumination properties. *ACS Applied Materials and Interfaces* 7, 14035 (**2015**).

22. K. J. Sankaran, B. R. Huang, A. Saravanan, D. Manoharan, N. H. Tai, and I. N. Lin, Nitrogen incorporated ultrananocrystalline diamond microstructures from bias-enhanced microwave N-2/CH4-plasma chemical vapor deposition. *Plasma Processes and Polymers* 13, 419 (**2016**).

23. T.-H. Chang, P.-Y. Hsieh, S. Kunuku, S.-C. Lou, D. Manoharan, K.-C. Leou, I.-N. Lin, and N.-H. Tai, High stability electron field emitters synthesized via the combination of carbon nanotubes and N2-plasma grown ultrananocrystalline diamond films. *ACS Applied Materials and Interfaces* 7, 27526 (**2015**).

24. R. Arenal, P. Bruno, D. J. Miller, M. Bleuel, J. Lal, and D. M. Gruen, Diamond nanowires and the insulator-metal transition in ultrananocrystalline diamond films. *Physical Review B* 75, 195431 (**2007**).

25. H. Kuzmany, R. Pfeiffer, N. Salk, and B. Günther, The mystery of the 1140 cm^{-1} Raman line in nanocrystalline diamond films. *Carbon* 42, 911 (**2004**).

26. A. Ferrari and J. Robertson, Origin of the 1150-cm^{-1} Raman mode in nanocrystalline diamond. *Physical Review B* 63, 121405 (**2001**).

27. R. Pfeiffer, H. Kuzmany, N. Salk, and B. Günther, Evidence for trans-polyacetylene in nanocrystalline diamond films from H-D isotropic substitution experiments. *Appl. Phys. Lett.* 82, 4149 (**2003**).

28. A. C. Ferrari and J. Robertson, Resonant Raman spectroscopy of disordered, amorphous, and diamond like carbon. *Physical Review B* 64, 075414 (**2001**).

29. A. C. Ferrari and J. Robertson, Interpretation of Raman spectra of disordered and amorphous carbon. *Physical Review B* 61, 14095 (**2000**).

30. H. Y. Yue, S. Huang, J. Chang, C. Heo, F. Yao, S. Adhikari, F. Gunes, L. C. Liu, T. H. Lee, E. S. Oh, B. Li, J. J. Zhang, T. Q. Huy, N. V. Luan, and Y. H. Lee, ZnO nanowire arrays on 3D hierachical graphene foam: Biomarker detection of Parkinson's disease. *ACS Nano* 8, 1639 (**2014**).

IP: 178.57.67.42 On: Sat, 02 Feb 2019 10:01:20
Copyright: American Scientific Publishers
Delivered by Ingenta